LIMIT EQUILIBRIUM AS BASIS FOR DESIGN OF GEOSYNTHETIC REINFORCED SLOPES

By Jorge G. Zornberg,[1] Nicholas Sitar,[2] Members, ASCE, and James K. Mitchell,[3] Honorary Member, ASCE

ABSTRACT: Limit equilibrium methods are evaluated with respect to their ability to predict failure of geosynthetic reinforced slope models tested in a geotechnical centrifuge. The variables considered in the centrifuge testing program were the reinforcement spacing, reinforcement tensile strength, and soil shear strength. Extensive testing was initially conducted to evaluate the strength properties under operational conditions of the backfill material, the model geotextile reinforcements, and the several interfaces in the slope models. Parametric studies were performed to evaluate the effect of the in-soil geotextile tensile strength, nonuniformity of unit weight in the centrifuge models, orientation of reinforcement forces, reinforcement overlapping layers, lateral friction of the models against centrifuge box, and selected method of slope stability analysis. All centrifuge slope models built using the same backfill soil yield a single Normalized Reinforcement Tension Summation. This normalized value can be interpreted as an earth pressure coefficient that depends on the soil friction angle and on the slope inclination. The evaluation also indicates that limit equilibrium should consider horizontal orientation of reinforcement forces, that significant contribution to stability is provided by the overlapping reinforcement layers, and that different rigorous limit equilibrium methodologies provide equally good results. Very good agreement was obtained between the g-levels at failure obtained experimentally and those predicted by limit equilibrium. Equally good agreement was obtained between experimental and predicted locations of the failure surfaces.

INTRODUCTION

Limit equilibrium methods have been traditionally used to analyze the stability of slopes with and without reinforcements. As limit equilibrium predictions of the performance of geosynthetic reinforced slopes have not been fully validated against monitored failures, a centrifuge study was initiated to evaluate the assumptions and selection of parameters for design of these structures.

A series of reinforced slope models was built as part of the centrifuge testing program using nonwoven geotextiles as reinforcement elements. All models were built with a 1H:2V slope inclination and were subjected to increasing centrifugal acceleration until failure occurred. Failure of the models was characterized by well-defined shear surfaces through the toe of the slopes. However, in contrast to the current design assumptions that failure should initiate at the toe of the reinforced slopes, failure initiated at midheight of the slopes. The experimental results also indicated that failure occurred due to breakage of the reinforcements without evidence of pullout, and that failure was controlled by the soil peak shear strength instead of by the critical state shear strength (Zornberg et al. 1998).

Building upon these experimental observations, the purpose of this paper is to further evaluate the results of the centrifuge testing program in order to investigate the validity of the limit equilibrium method as a basis for design of geosynthetic reinforced soil slopes. To this effect, an assessment of the strength properties under operational conditions of the backfill soil, the geotextile reinforcement, and the several interfaces in the slope models is initially presented. Then, different assumptions in the limit equilibrium analysis of geosynthetic reinforced soil slopes are evaluated, and a comparison between experimental results and limit equilibrium predictions is presented. Finally, normalization of the centrifuge test results and its implications on the design of geosynthetic reinforced soil structures are discussed.

CENTRIFUGE TESTING PROGRAM

All reinforced slope models in this experimental testing program were built with the same slope inclination (1H:2V) and the same total height (254 mm). Fig. 1 shows the reinforcement layout and typical instrumentation in a reinforced slope model. The models were built using sand as backfill material and nonwoven fabrics as reinforcing elements. The models were subjected to a progressively increasing centrifugal acceleration until failure occurred. A detailed description of the characteristics of the centrifuge testing program is presented by Zornberg et al. (1998). The centrifuge tests can be grouped into three test series (B, D, or S). Accordingly, each reinforced slope model in this study was named using a letter that identifies the test series, followed by the number of reinforcement layers in the model. Each test series aimed at investigating the effect of one variable, as follows:

- *Baseline, B-series*: performed to investigate the effect of the reinforcement vertical spacing. Centrifuge models in this series were built with six, nine, 12, and 18 reinforcement layers.
- *Denser soil, D-series*: performed to investigate the effect of the soil shear strength on the stability of geosynthetic reinforced slopes. The models in this series were built with a denser backfill sand but with the same reinforcement type as in the B-series.
- *Stronger geotextile, S-series*: performed to investigate the effect of the reinforcement tensile strength on the performance of reinforced slopes. The models in this series were built using reinforcements with a higher tensile strength than in the B-series but with the same backfill density as in that series.

MATERIAL PROPERTIES

Proper evaluation of the material and interface strength properties that influence the performance of the centrifuge

[1]Asst. Prof., Dept. of Civ., Envir., and Arch. Engrg., Univ. of Colorado, Boulder, CO 80309; formerly, Proj. Engr., Geo Syntec Consultants, Huntington Beach, CA 92648.

[2]Prof., Dept. of Civ. and Envir. Engrg., Univ. of California, Berkeley, CA 94720.

[3]Univ. Distinguished Prof. and Via Prof. of Civ. Engrg., Virginia Polytechnic Inst. and State Univ., Blacksburg, VA 24061-0105.

Note. Discussion open until January 1, 1999. Separate discussions should be submitted for the individual papers in this symposium. To extend the closing date one month, a written request must be filed with the ASCE Manager of Journals. The manuscript for this paper was submitted for review and possible publication on December 26, 1996. This paper is part of the ***Journal of Geotechnical and Geoenvironmental Engineering***, Vol. 124, No. 8, August, 1998. ©ASCE, ISSN 1090-0241/98/0008-0684–0698/$8.00 + $.50 per page. Paper No. 14817.

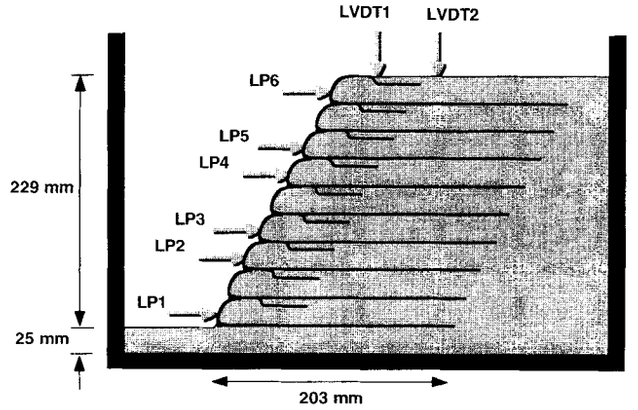

FIG. 1. Centrifuge Model with 25.4 mm Reinforcement Spacing [Linear Potentiometers (LPs) and Linear Variable Displacement Transducers (LVDTs) Are Indicated in Figure]

models at failure was required to assess the predicting capabilities of limit equilibrium stability analysis. Consequently, a testing program was carried out to evaluate the shear strength of the sand used as backfill material, the tensile strength of the model geotextiles used as reinforcement, and the shear strength of the interfaces between the backfill and reinforcements and between the backfill and the centrifuge box. These properties were estimated for the most representative conditions in the slope models in order to accurately predict their failure. Accordingly, the shear strength of the sand was estimated for plane strain conditions and the tensile strength of the geotextiles was evaluated under embedment conditions.

Backfill

The model slopes were built using Monterey No. 30 sand, which is a clean, uniformly graded sand classified as SP in the Unified Soil Classification System. The particles are rounded to subrounded, consisting predominantly of quartz with a smaller amount of feldspars and other minerals. The average particle size for the material is 0.4 mm, the coefficient of uniformity is 1.3, and the coefficient of curvature is about 1.1. The maximum and minimum void ratios of the sand are 0.83 and 0.53, respectively. To obtain the target dry densities in the model slopes, the sand was pluviated through air at controlled combinations of sand discharge rate and discharge height. The unit weights for the Monterey No. 30 sand at the target relative densities of 55 and 75% are 15.64 and 16.21 kN/m^3, respectively.

Two series of triaxial tests were performed to evaluate the friction angle for the Monterey No. 30 sand as a function of relative density and of confining pressure. The tests were performed using a modified form of the automated triaxial testing system developed by Li et al. (1988). The specimens had nominal dimensions of 70 mm in diameter and 150 mm in height and were prepared by dry tamping. Fig. 2(a) shows the increase in peak friction angle with increasing relative density at a confining pressure of 100 kPa. Of particular interest are the friction angles obtained at relative densities of 55 and 75%, which correspond to the relative density of the backfill material in the models. The estimated triaxial compression friction angles (ϕ_{tc}) at these relative densities are 35° and 37.5°, respectively. Although the tests did not achieve strain values large enough to guarantee a critical state condition, the friction angles at large strains appear to converge to a critical state value (ϕ_{cs}) of approximately 32.5°. This value agrees with the critical state friction angle for Monterey No. 0 sand obtained by Riemer (1992). As the critical state friction angle is mainly a function of mineralogy (Bolton 1986), Monterey No. 0 and Monterey No. 30 sands should show similar ϕ_{cs} values. Fig.

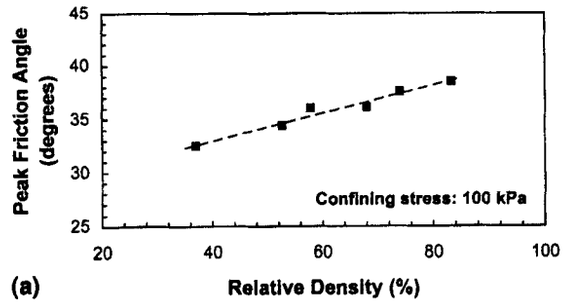

FIG. 2(a). Friction Angle for Monterey No. 30 Sand Obtained from Triaxial Testing at Different Relative Densities

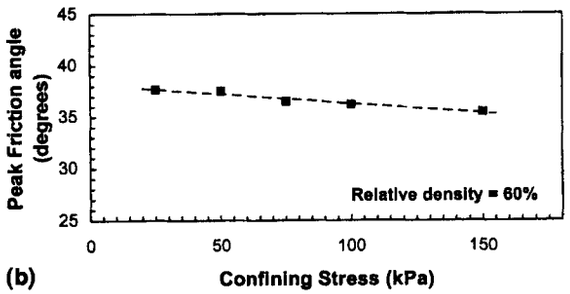

FIG. 2(b). Friction Angle for Monterey No. 30 Sand Obtained from Triaxial Testing at Different Confining Pressures

2(b) presents the effect of confining pressure on the frictional strength of the sand at an approximate relative density of 60%. These results show that the friction angle of Monterey No. 30 decreases only slightly with increasing confinement. The fact that the friction angle of this sand does not exhibit much normal stress dependency avoids additional complications in the interpretation of the centrifuge model tests.

Of particular interest in this study is the effect of the intermediate effective principal stress under plane strain conditions, which has been found to increase the peak friction angle of sand relative to that measured in conventional triaxial compression tests (Ladd et al. 1977). Plane strain is the prevailing condition in reinforced soil structures [e.g., Jewell (1990)], and friction angles for this condition had been considered in previous centrifuge studies that evaluated the performance of reinforced soil walls (Jaber 1989). Considering the experimental difficulties involved in accurately evaluating plane strain friction angles (ϕ_{ps}), these values were inferred based on correlations with the friction angles obtained under triaxial compression conditions (ϕ_{tc}). Specific correlations for the sand used in this study were obtained from results of plane strain tests performed using Monterey sands. Lade and Duncan (1973) reported plane strain friction angles for Monterey No. 0 sand, obtained from true triaxial tests on cubical specimens. Additionally, Marachi et al. (1981) reported the results of a series of tests on Monterey No. 20 sand obtained using triaxial and plane strain devices. The friction angle ratios ϕ_{ps}/ϕ_{tc} for Monterey No. 0 and Monterey No. 20 sands are indicated in Fig. 3. The friction angle ratios for the two Monterey sands increase with increasing relative density of the sand. Based on this correlation, the ratios ϕ_{ps}/ϕ_{tc} used in this study for Monterey No. 30 sand at 55 and 75% relative densities are 1.13 and 1.14, which yields plane strain friction angles of 39.5° and 42.5°, respectively.

The average strength increase ratio recommended by Kulhawy and Mayne (1990) is

$$\phi_{ps} = 1.12\phi_{tc} \tag{1}$$

which is in good agreement with the correlation obtained specifically for Monterey sands and provides additional confidence in the plane strain values selected in the current study.

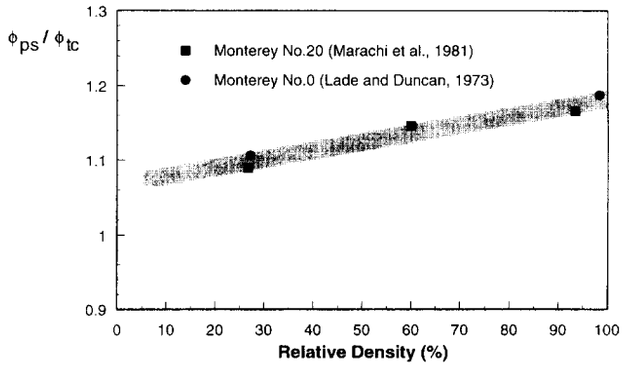

FIG. 3. Ratio of Friction Angles under Plane Strain and Triaxial Compression Conditions for Monterey Sand

Geotextile Reinforcements

Two types of nonwoven fabrics, which are used for interfacing purposes, were selected as reinforcements for the centrifuge slope models. The weaker of these fabrics (Pellon Sew-In nonwoven) is a white, 100% polyester fabric with a mass per unit area of 24.5 g/m^2. The stronger of the fabrics (Pellon Tu-Grid nonwoven) is a white 60% polyester/40% rayon fabric with blue 25-mm square grid prints and a mass per unit area of 28 g/m^2. The remainder of this paper refers to the weaker model reinforcement as "Geotextile W" and to the stronger reinforcement as "Geotextile S." Prototype geotextiles with a mass per unit area almost 100 times higher than in the model geotextiles are available in the geosynthetics market. Consequently, models tested under accelerations as high as $100g$ would still be representative of structures built using prototype geotextile reinforcements. The tensile strength of the model reinforcements is highly anisotropic, with the lower strength in the cross-machine direction. As the model slopes should reach failure within the capacity of the centrifuge, the fabrics were oriented during construction of the models so that their weak, cross-machine direction will be loaded during testing.

The ASTM D4595 wide-width strip tensile test uses an unconfined 200 mm wide specimen that is 100 mm long between the faces of the opposing grips. However, the geosynthetic mechanical properties should be measured in a manner that simulates the confined field conditions. Several studies have shown that geotextiles (particularly nonwovens) have higher stiffness and tensile strength under soil confinement (McGown et al. 1982; Ling et al. 1992; Zornberg and Mitchell 1994). The increase in confinement caused by soil embedment has been generally identified as the main cause for the improvement in the geotextile mechanical properties. However, there are actually two possible causes of improvement:

1. Embedment of nonwoven geotextiles in soil provides confinement which increases the geotextile tensile strength.
2. Embedment of nonwoven geotextiles in soil restrains geotextile deformations in the direction perpendicular to loading which increases the geotextile tensile strength.

The boundary conditions in unconfined wide-width testing of nonwoven geotextiles may not be representative of field conditions since, due to Poisson's ratio effect, the specimens may undergo severe "necking" under increased loading. Although wide enough specimens may provide negligible lateral deformations, the size of the geotextile specimen that restrains necking is not clearly defined. While the 2:1 width/length specimen ratio has been considered reasonable for unconfined tests by some investigators (Shrestha and Bell 1982), larger 5:1 ratios have also been recommended (Leflaive et al. 1982), and tests have been even performed using a gauge length of only 3 mm (Resl 1990). In general, lightweight nonwoven geotextiles have been found to be more sensitive to the width/length ratio of the specimen.

A series of wide-width strip tensile tests ASTM D4595 was performed to evaluate the unconfined tensile strength properties of the model geotextiles in their cross-machine direction. The conventionally specified crosshead speed of 10 mm/min was used in the tests. The unconfined ultimate tensile strength (i.e., the peak or maximum unit tension) and the strain at ultimate strength for Geotextile W were 0.063 kN/m and 17.7%, respectively. The unconfined ultimate tensile strength and the strain at ultimate strength for Geotextile S were 0.119 kN/m and 29.3%, respectively. The strain at ultimate strength obtained for these two model geotextiles is consistent with values obtained from wide-width testing for prototype nonwoven geotextiles. Fig. 4 shows typical unit tension versus strain curves for these materials. A softening postpeak behavior is observed in both geotextiles.

Model geotextile specimens with decreasing gauge lengths were also tested in order to evaluate the effect of testing boundary conditions on the estimated tensile strength. For very large width/length ratios the tests approximate a condition in which lateral deformations are negligible. All tensile tests were performed on 200 mm wide specimens, and the gauge length was decreased from the standard 100 mm length to as little as 1.5 mm. The adoption of a very small gauge length was motivated by observation of the failure pattern in model geotextiles retrieved after centrifuge testing. Reinforcements retrieved from the models after failure showed clear breakage lines perpendicular to the loading direction without visible signs of stretching at either side of the tear. Fig. 5 shows a model geotextile retrieved after centrifuge testing (center of the figure), as well as specimens obtained after standard wide-width tensile testing, and after testing using the 1.5 mm gauge length setup. It appears that the breakage pattern in the geotextile retrieved from the slope model resembles that of the specimen tested using the smaller gauge length.

The tensile strength obtained for Geotextile W when tested using a 1.5 mm gauge length setup was 0.150 kN/m, with an approximate displacement at peak tension of 1.3 mm. This tensile strength is 137% higher than the value obtained from standard wide-width testing. Fig. 6 shows the unit tension versus displacement curve for one of the Geotextile W specimens. As was also the case in the standard wide-width test results, a marked postpeak softening behavior was observed in these tests. For the Geotextile S, the ultimate tensile strength obtained using a 1.5 mm gauge length was 0.234 kN/m with an average displacement at peak tension of 2.5 mm. This tensile strength is 97% higher than the ultimate strength from wide-

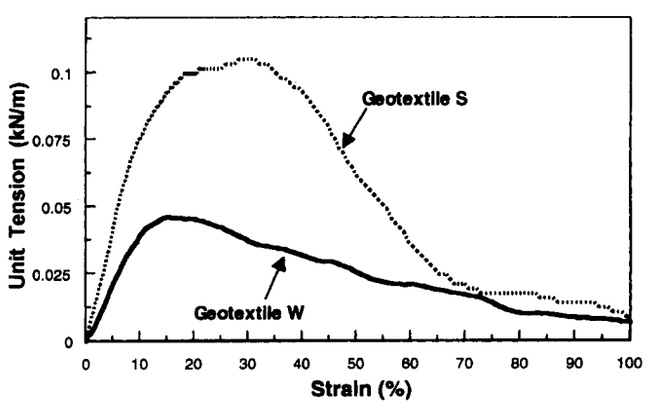

FIG. 4. Typical Wide-Width Tensile Test Results for Geotextile Reinforcements

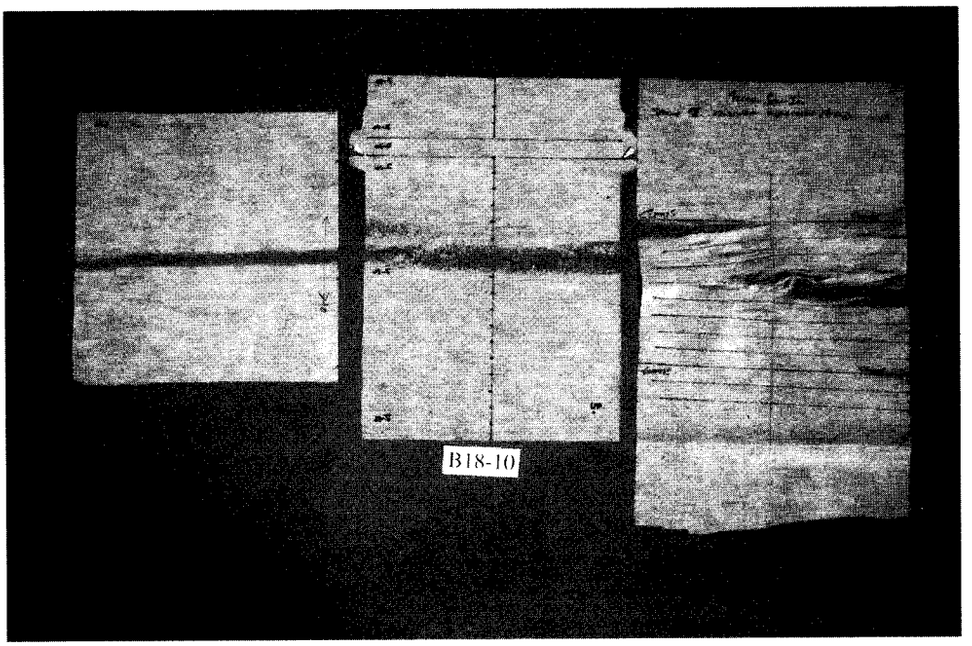

FIG. 5. Breakage Pattern in Geotextile Specimens Tested Using (from Left to Right) Small Gauge Length Setup, Centrifuge Modeling, and Standard Wide-Width Testing

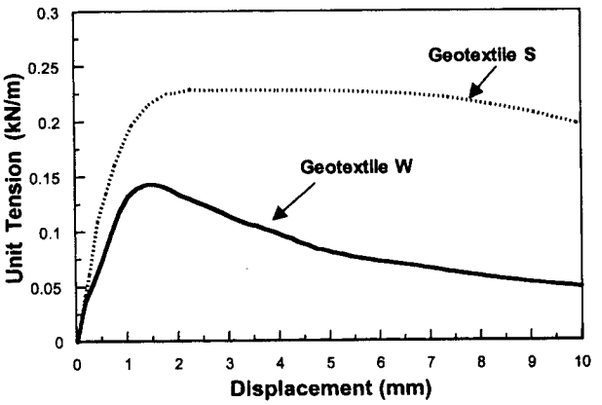

FIG. 6. Typical Tensile Test Results for Model Geotextiles Obtained Using Small Gauge Length Setup

width testing. A typical unit tension versus displacement curve for a Geotextile S specimen is also shown in Fig. 6. While a softening behavior was observed in the wide-width tests, postpeak softening did not occur in the small gauge length tests. The difference in postpeak behavior between Geotextile W and Geotextile S materials, as observed only from tensile tests performed using small gauge length, is relevant to the postfailure performance of the centrifuge models (Zornberg et al. 1998).

Interface Properties

Direct shear tests were performed to evaluate the interface shear strength between the sand and each of the two model geotextiles used as reinforcements. Direct shear tests were also performed to determine the interface strength between the sand and the Teflon and Mylar materials that lined the walls of the centrifuge box. The geotextile, Teflon, and Mylar specimens were mounted to a 100-mm-diameter steel base platen. The sand material was then placed above this base platen within a 50 × 50 mm square steel forming mold. The procedures for direct shear testing were based on those followed during investigation of interface strength parameters for the Kettleman Hills waste landfill slope failure (Mitchell et al. 1990). In that study, good agreement was found between the residual interface shear strength properties measured in the small direct shear apparatus and in larger pullout tests. This adds confidence to the use of the simpler direct shear tests for determination of interface strength.

The tests were carried out under strain-controlled loading using sand specimens at a relative density of about 60%. Normal pressures on the specimen interfaces were selected to be representative of the stresses experienced in the centrifuge tests. Fig. 7 shows the interface test results for Geotextile W and Geotextile S, tested under a normal pressure of 85 kPa. The results are plotted as mobilized friction angle versus shear displacement. The interfaces between Monterey No. 30 sand and both model geotextiles show a similar behavior, achieving a peak strength at approximately 1.5 mm of shear displacement. No marked postpeak softening behavior is observed for any of the two interfaces.

For plane sheet materials such as geotextiles, the direct sliding resistance obtained from direct shear tests governs the anchorage length required to mobilize the allowable reinforcement force. For practical purposes, the strength of the sand/geotextile interfaces can be characterized by the interface friction factor f, defined as

$$f = \frac{\tan \delta}{\tan \phi} \tag{2}$$

where δ = interface friction angle; and ϕ = soil friction angle. The interface friction factor for the model geotextiles in this study, as defined using direct shear measurements for both δ and ϕ, is approximately 0.9.

The interface friction between the sand and the Teflon and Mylar materials used to line the walls of the centrifuge box was also determined. The tests were performed using sand placed at a 60% relative density. Test results on both interfaces indicate that the peak strength develops at very small shear displacements (less than 0.25 mm), with the sand/Teflon interface showing a higher residual strength than the sand/Mylar interface. Table 1 summarizes the results of the interface direct shear tests.

LIMIT EQUILIBRIUM

The limit equilibrium method (Terzaghi 1956) still remains the most widely used approach to obtain approximate solutions

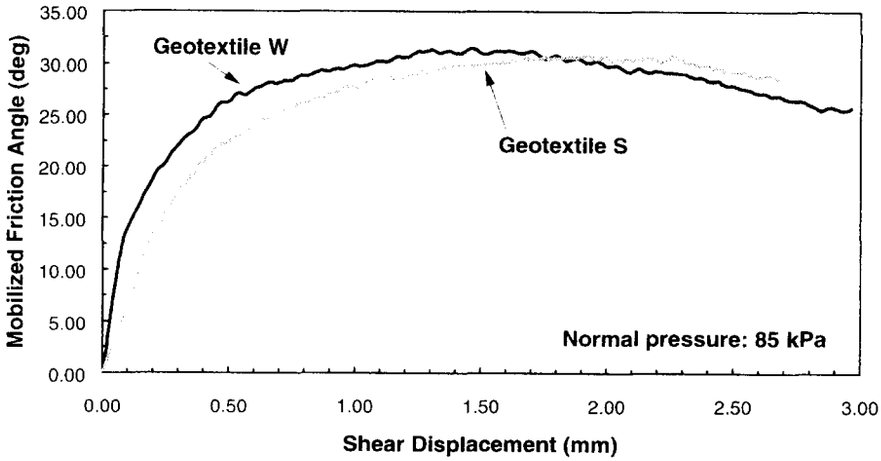

FIG. 7. Direct Shear Test Results for Sand/Geotextile Interfaces

TABLE 1. Direct Shear Test Results

Interface (1)	Average normal pressure (kPa) (2)	Peak friction angle (degrees) (3)	Shear displacement at peak (mm) (4)	Residual friction angle (degrees) (5)
Sand/Geotextile W	61	33.5	1.78	—
	85	31	1.37	—
Sand/Geotextile S	71	30.5	1.27	—
	85	30.5	1.68	—
Sand/Mylar	69	13.5	0.15	11
Sand/Teflon	72	19	0.23	18

for complex stability problems. Limit equilibrium analysis of unreinforced structures includes assumptions that are also needed when analyzing reinforced soil slopes (e.g., the shape of the failure surface). Additional assumptions that are needed for the analysis of reinforced slopes include the inclination (e.g., horizontal, tangential) and distribution of the reinforcement tensile forces along the selected failure surface (e.g., linear, constant with depth). The failure surfaces most widely used in the limit equilibrium analysis of reinforced soil slopes include the planar wedge [e.g., Schlosser and Vidal (1969)], the bilinear wedge surface [e.g., Jewell (1991)], the logarithmic spiral [e.g., Leshchinsky and Boedeker (1989)], and the circular surface [e.g., Wright and Duncan (1991)]. Several of the analysis methods have evolved into design charts used to determine the reinforcement requirements for simple slopes.

Although different definitions for the factor of safety have been reported for the design of reinforced soil slopes, the definition used in this study is relative to the shear strength of the soil:

$$FS = \frac{\text{Available soil shear strength}}{\text{Soil shear stress required for equilibrium}} \quad (3)$$

This definition is consistent with conventional limit equilibrium analysis, for which extensive experience has evolved for the analysis of unreinforced slopes.

Current design practices for reinforced soil slopes often consider approaches that decouple the soil reinforcement interaction and do not strictly consider the factor of safety defined in (3). Such analyses neglect the influence of reinforcement forces on the soil stresses along the potential failure surface and may result in factors of safety significantly different than those calculated using more rigorous approaches. Different rigorous methods of analysis have been developed for the analysis of geosynthetic reinforced slopes (Leshchinsky and Boedeker 1989; Jewell 1991; Wright and Duncan 1991). A rigorous internal stability method for circular surfaces (Spencer's) as coded in the computer program UTEXAS3 (Wright 1990) was used in this study for the analysis of the centrifuge slope models. The experimental centrifuge test results are also compared to those predicted using design charts based on other rigorous limit equilibrium approaches.

EVALUATION OF MODELING ASSUMPTIONS IN LIMIT EQUILIBRIUM

The effect on the limit equilibrium results of the geotextile tensile strength, orientation of the reinforcement forces, reinforcement overlaps, nonuniform acceleration in centrifuge models, friction at model boundaries, and selected method of analysis were investigated. Parametric studies were performed for model B18, which failed at $76.5g$. The limit equilibrium analyses were performed by searching for the critical circular surface, instead of adopting a fixed circle matching the observed failure surface. Based on the interpretation of the experimental results regarding the performance of the reinforced slope models at failure, the peak friction angle (instead of the critical state friction angle) was adopted to characterize the shear strength of the backfill sand. Also based on the experimental observations, a uniform distribution of maximum reinforcement forces with depth (instead of a triangular distribution) was used in the analyses [see Zornberg et al. (1998)].

Effect of Geotextile Tensile Strength

The geotextile testing program described before suggested that the in-soil geotextile tensile strength is higher than the strength obtained from standard unconfined wide-width tensile tests. Although evidence of improvement due to confinement in the geotextile mechanical properties is apparent, current testing procedures do not accurately quantify this improvement. The alternative is to evaluate the in-situ geotextile tensile strength by back calculation from one of the centrifuge models reinforced with each of the two geotextile types used in this investigation. Based on the inferred distribution of maximum reinforcement forces with depth at the moment of failure (Zornberg et al. 1998), a constant ultimate tension at failure, T_{ult}, can be back calculated for the purposes of the analyses presented herein. This back calculated tensile strength corresponds to the average reinforcement tension with depth at the moment of failure.

Fig. 8 shows the calculated factors of safety as a function of geotextile strength and centrifuge acceleration. The results show an approximately linear increase in the value of calculated factors of safety with increasing reinforcement strength

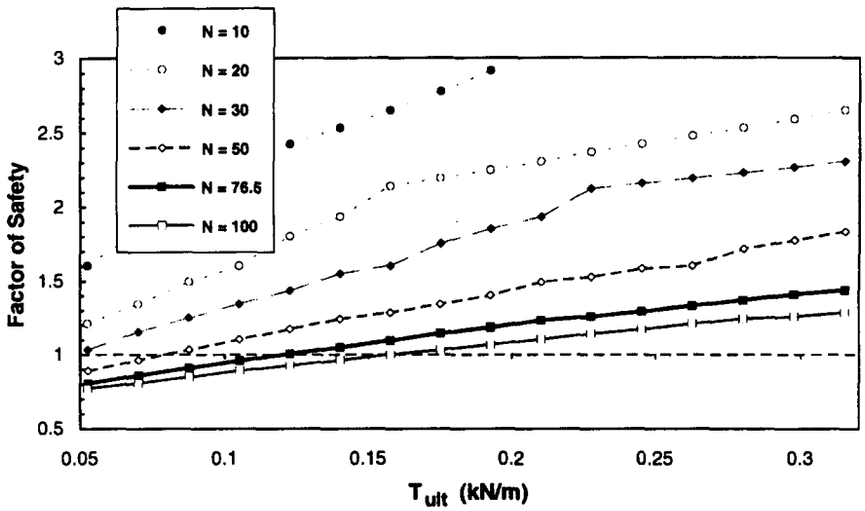

FIG. 8. Effect of Geotextile Strength on Calculated Factor of Safety for Model B18 (N = Number of g-Levels)

at each g-level N. Of particular interest is the curve that corresponds to the g-level at failure obtained experimentally from centrifuge testing ($N = N_f = 76.5g$). At this centrifugal acceleration, the back calculated geotextile strength T_{ult} is the value that yields a FS of unity. For the Geotextile W used as reinforcement in model B18, the back calculated geotextile strength is approximately T_{ult} = 0.123 kN/m. This value was adopted as the in-soil tensile strength for the limit equilibrium analysis of models built using Geotextile W as reinforcement elements. Based on a similar back analysis using model S9, the estimated in-soil tensile strength for the Geotextile S is 0.184 kN/m.

Fig. 9 summarizes the results of the testing program carried out to evaluate the tensile strength of the geotextiles used in the centrifuge models. The figure shows the tensile strength results obtained for different width/length ratios for Geotextile W and Geotextile S. The results for the width/length ratios of 2 and 133 (100 mm and 1.6 mm gauge lengths) are the average results obtained from three tensile tests. The intermediate results were obtained from a single test. All tests were performed at a crosshead speed of 10 mm/min. Fig. 9 provides a range of possible tensile strength values that could be adopted in the analysis of the reinforced slope models. As mentioned, the geotextile strength values finally selected herein were obtained by back calculating the results of one centrifuge slope built using each geotextile type. The in-soil tensile strength values back calculated by limit equilibrium are also indicated in the figure. The back calculated values fit well within the range obtained in the geotextile testing program.

The back calculated strength values are lower than those obtained using the 1.5 mm gauge length tensile tests. Two different explanations can be offered in order to characterize the geotextile strength properties, regarding the "actual" in-soil geotextile tensile strength:

1. The "actual" in-soil strength is the value obtained from tensile testing using a small gauge length. The smaller strength value obtained from back analysis of centrifuge tests may be due to the fact that the distribution of reinforcement forces is not uniform with depth as assumed in the analyses.
2. The "actual" in-soil strength is the value obtained from back analysis of centrifuge tests considering a uniform reinforcement force distribution with depth. The strength value obtained from tensile tests with small gauge length is higher due to the effect of the strain rate on the test results.

Although the in-soil geotextile tensile strength values were eventually selected using results from two centrifuge tests, it is important to note that these values were not blindly predicted from back calculation. The possible range for in-soil tensile strength values was defined from the geotextile tensile testing program, and these results were refined using information from centrifuge tests. This procedure was adopted for selection of the reinforcement tensile strength considering the difficulty in quantifying experimentally the in-soil mechanical properties of low-strength nonwoven fabrics.

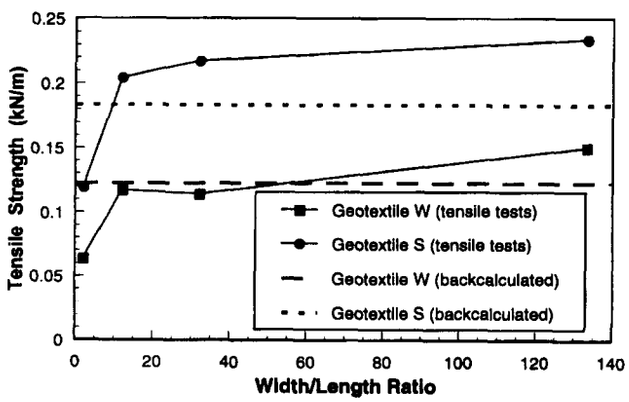

FIG. 9. Tensile Strength of Model Geotextiles as Function of Width/Length Ratio of Specimen

Effect of Orientation of Reinforcement Forces

The orientation of the reinforcement forces must be assumed in the limit equilibrium analysis of reinforced soil slopes. The inclination of the tensile forces has been assumed in current practice to vary between horizontal (as-installed) and tangent to the potential slip surface. In-flight observation of the reinforced slope models at increasing accelerations suggests that the orientation of the reinforcements was not tangent to the failure surface and that the reinforcements remained horizontal until the moment of failure. This is consistent with results from laboratory and analytical studies of soil shear zone formation (Shewbridge and Sitar 1989). Although the experimental observations indicated that reinforcement forces should be considered horizontal in the analyses, a parametric evaluation was made on the effect of reinforcement orientation on the calculated factors of safety.

Fig. 10 shows the factors of safety for model B18 calculated with increasing accelerations considering horizontal and tan-

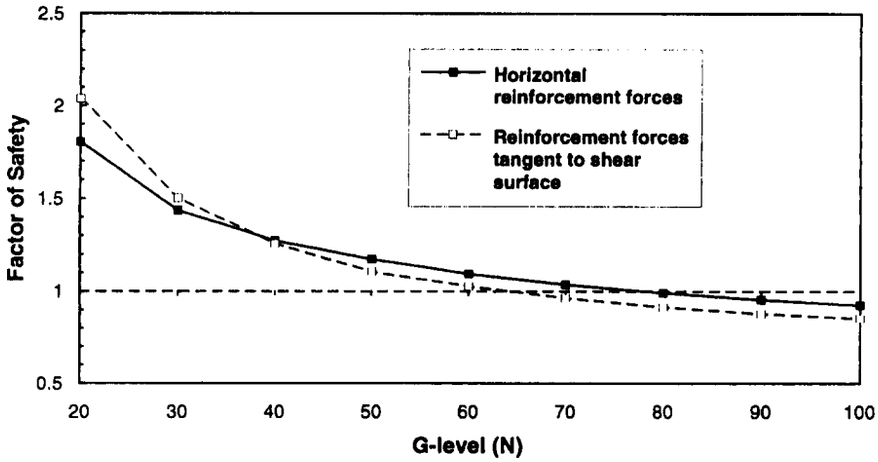

FIG. 10. Calculated Factors of Safety for Model B18 with Increasing Acceleration: Effect of Orientation of Reinforcement Forces

gential reinforcement forces. The figure shows that only small differences are obtained in the calculated factors of safety (less than 10% difference). The results of these analyses indicate that the use of horizontal reinforcement forces would be a conservative assumption for overdesigned slopes (high FS), while it would be unconservative for the case of underdesigned structures (low FS). For factors of safety typically adopted in design (e.g., 1.3 to 1.5) the orientation of reinforcement forces for cohesionless fills has little effect on the factors of safety, as long as calculations are performed using rigorous limit equilibrium methods. These results are in agreement with previous studies on the effect of reinforcement orientation (Leshchinsky and Boedeker 1989; Wright and Duncan 1991). A reinforcement force tangential to the failure surface produces a larger stabilizing moment than a horizontal force, but it has a smaller influence on the normal forces (and consequently on the soil shear strength contribution) along the shear surface. Since the effect of the two contributions to stability (i.e., reinforcement tension and soil shear strength) tend to compensate for each other, the net effect of the selected reinforcement force orientation is thus small.

Effect of Geotextile Overlaps

The model geotextiles were wrapped around the slope face of the models during construction (Fig. 1). Current design of geosynthetic reinforced slopes does not take into account the contribution of reinforcement overlapping to the internal stability of the structure. However, the geotextile overlaps worked as additional reinforcements in the centrifuge models. The overlaps intersected by the failure surface near the base of the centrifuge models failed by breakage, without signs of pullout (Zornberg et al. 1998). Based on this experimental evidence, the overlaps were modeled as additional short reinforcement layers in the limit equilibrium analyses performed in this study.

Fig. 11(a) illustrates the effect of the reinforcement overlaps on the limit equilibrium results. The figure shows the factors of safety calculated for model B18 with increasing accelerations. A total of 18 primary reinforcement layers were used in a first set of analyses that did not consider the overlaps. A total of 36 reinforcements (equal number of primary and secondary layers) were used in a second set of analyses that modeled the overlapping layers. The figure shows that the geotextile overlaps contributed to the stability of the slope by increasing the factor of safety by an approximately constant value ($\Delta FS \approx 0.12$) at the different g-levels. Although disregarding the effect of overlaps may be a conservative assumption for design, their contribution must be taken into account to correctly predict failure of the centrifuge models.

Moreover, neglecting the effect of geotextile overlaps is apparently an unconservative assumption regarding the location of the critical failure surface. Fig. 11(b) compares the critical circles obtained from limit equilibrium analyses performed to investigate the effect of reinforcement overlaps. The critical circle obtained using the experimental acceleration at failure for model B18 ($N_f = 76.5g$) and taking the geotextile overlaps into account matches the failure surface obtained experimen-

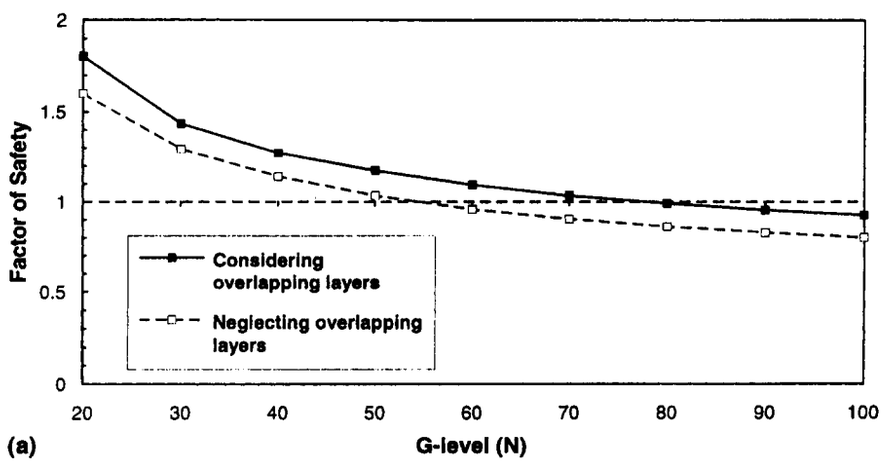

(a)

FIG. 11(a). Calculated Factors of Safety for Model B18 with Increasing Acceleration: Effect of Geotextile Overlaps

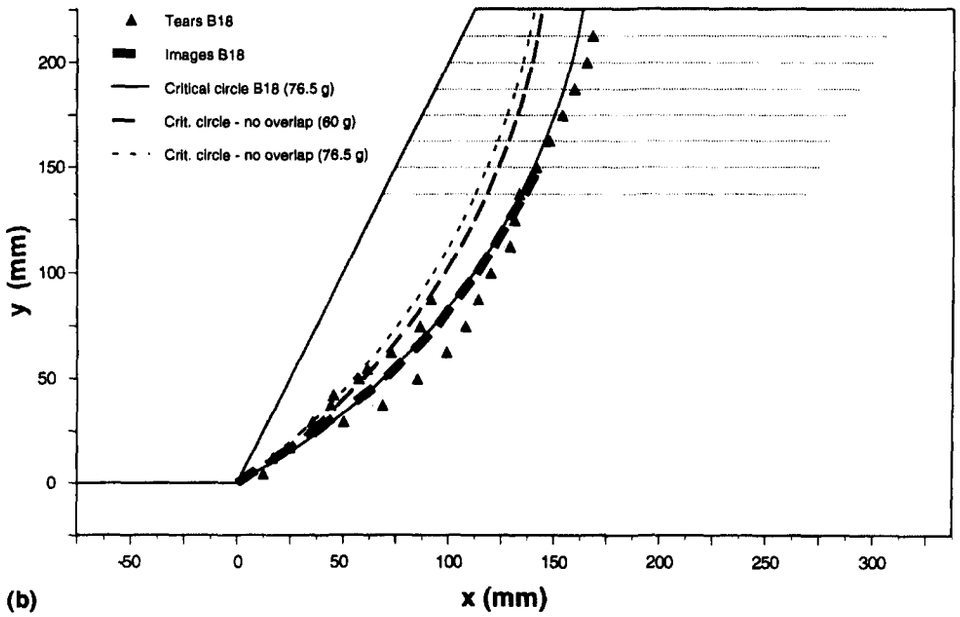

FIG. 11(b). Effect of Geotextile Overlaps on Predicted Critical Circles

tally. For comparison, two critical circles obtained for analyses that did not model the overlaps are shown: the critical circle obtained using the acceleration that yields a factor of safety of unity ($N = 60g$), and the critical circle obtained using the experimental g-level that induced the model failure ($N_f = 76.5g$). The critical circles obtained in analyses that do not model the overlaps are closer to the slope face. Consequently, the reinforcement embedment lengths could be unconservatively estimated if the analyses were performed without modeling the reinforcement overlaps.

Effects of Nonuniform Unit Weight and of Friction at Model Boundaries

The acceleration within a centrifuge model increases linearly with depth, proportionally to the radius of rotation. The effect of increasing acceleration with radius in the model slopes was investigated by comparing the factors of safety calculated considering a constant unit weight to those calculated considering an increasing unit weight with depth in the model. Very good agreement was obtained between the two sets of results, showing that the assumption regarding the nonuniformity of the unit weight has a negligible effect in the estimated factors of safety (Zornberg et al. 1995).

The effect of friction at model boundaries was observed to be negligible because (1) The breakage pattern of the geotextiles showed no curvature toward the edges; (2) the horizontal displacements observed through the Plexiglas side wall compared well with those observed within the soil mass (as evaluated in a model wetted and dissected after testing); and (3) the failure surface defined from the location of geotextile tears showed good agreement with the surface defined from images recorded through the Plexiglas side wall. However, friction angles estimated using direct shear tests representing the model boundaries (sand/Teflon and sand/Mylar interfaces) were not negligible. Consequently, a parametric study was performed to investigate the effect of the lateral friction on the calculated factors of safety. The results indicated that the effect of lateral friction on the calculated factor of safety was small (on the order of 3%), and that this effect is probably accounted for in the analyses by using plane strain friction angles (Zornberg et al. 1995). Therefore, this effect was not included in the limit equilibrium analyses.

Influence of Selected Method of Slope Stability Analysis

The factors of safety for the centrifuge models were calculated using Spencer's method (Spencer 1967). This method satisfies all conditions of equilibrium and assumes that the interslice forces are parallel. For practical design of unreinforced slopes, it has been shown that methods that satisfy all conditions of equilibrium are accurate for any conditions, except when numerical problems are encountered. The maximum difference between factors of safety computed by any of these methods is no more than 12%. Thus, with an accuracy of ±6%, factors of safety calculated for unreinforced slopes by methods that satisfy all conditions of equilibrium can be considered to be the correct answer (Duncan 1996).

A difference in the calculated factor of safety of 6%, which may be acceptable for design purposes, may become significant when predicting the g-level at failure in the centrifuge slope models. A parametric study was then performed to evaluate the influence of the selected slope stability method on the calculated factors of safety. Since no code was available for limit equilibrium analysis of reinforced soil slopes using different rigorous methods, a thorough evaluation was not possible. However, good evidence that the different limit equilibrium methods would render very similar results was obtained by simulating the reinforcement forces as pseudostatic seismic forces.

An unreinforced slope with the same geometry and soil properties as model B18 was used for this evaluation. Using Spencer's method, the pseudostatic seismic coefficient that simulates the effect of the reinforcements in model B18 was estimated such that it yields a factor of safety of unity for the g-level causing failure. The calculated seismic coefficient was −0.205, which was then used in the remaining analyses. The computer program SLOPAS (Espinoza et al. 1992), which considers a variety of limit equilibrium methods and allows the use of pseudostatic seismic forces, was used in the analyses.

The various limit equilibrium methods make different assumptions regarding the direction of the resultant internal forces, the height of the line of thrust, or the shape of the distribution of internal shear forces. Table 2 compares the factors of safety calculated by different methods using the same critical circle. The factors of safety estimated using Spencer's

TABLE 2. Factors of Safety Calculated for Model B18 Using Different Limit Equilibrium Methods

Method (1)	Calculated factor of safety (2)
(*a*) Methods that satisfy all equilibrium equations	
Spencer (1967)	1.000
Morgenstern and Price (1965)	1.000
Sarma (1973)	1.000
Sarma (1979)	1.000
Janbu (1954)*	1.026
Correia (1988)	1.000
(*b*) Methods that do not satisfy all equilibrium equations	
Fellenius (1936)	0.780
Lowe and Karafiath (1960)	1.112
Bishop (1955)	1.000

*Janbu's method satisfies all equilibrium conditions except for the moment equilibrium of one slice.

and Bishop's methods were calculated using both UTEXAS3 and SLOPAS, which gave identical results. The rest of the analyses were performed using SLOPAS. The results in Table 2 indicate that all rigorous methods yield virtually the same factor of safety. Except for Janbu's method, which gave a factor of safety very close to 1.0, all other rigorous methods yielded exactly the same result up to the third decimal figure.

Additionally, three methods commonly used in geotechnical practice that do not satisfy complete static equilibrium were also evaluated. The Ordinary Method of Slices (Fellenius 1936), which only satisfies moment equilibrium, underestimates the factor of safety by more than 20%. Lowe and Karafiath's method, which satisfies both vertical and horizontal force equilibrium but does not satisfy moment equilibrium, overpredicts the factor of safety by more than 10%. Bishop's modified method, which satisfies moment and vertical force equilibrium, but does not satisfy horizontal force equilibrium, predicts the factor of safety as accurately as the rigorous methods, yielding a factor of safety of 1.000. The results obtained from this evaluation provide evidence that similar results would have been obtained in the limit equilibrium analyses of the centrifuge models using any of the indicated rigorous limit equilibrium methods or Bishop's method.

COMPARISON BETWEEN PREDICTED AND EXPERIMENTAL RESULTS

A major objective of the centrifuge testing program was to compare the experimental results with predictions using limit equilibrium analysis. Thus, after evaluating the modeling assumptions by analyzing model B18, limit equilibrium was used to predict the experimental results of the remaining models. The calculations were performed by searching for the critical circular surface, instead of adopting a fixed circle matching the observed failure surface. In this way, besides investigating the ability of limit equilibrium to predict the *g*-level at failure, the capability of the method for predicting the location of the failure surface could also assessed. Plane strain friction angles of 39.5° and 42.5° were used in the analyses for backfill at 55 and 75% relative densities, respectively. The geotextile tensile strengths used in the analyses were T_{ult} = 0.123 kN/m for Geotextile W and T_{ult} = 0.184 kN/m for Geotextile S.

The limit equilibrium analyses were performed considering a unit weight increasing with the centrifuge radius, uniform distribution of reinforcement forces with depth, horizontal orientation of reinforcement forces, and overlapping geotextile layers modeled as additional reinforcements. The effect of the wall friction at model boundaries was considered negligible and not accounted for in the analyses.

Experimental and Predicted *g*-Levels at Failure

The factors of safety calculated with increasing accelerations for the centrifuge slope models in the B-series are plotted in Fig. 12. For a given model, the factor of safety against failure decreases as the *g*-level increases. The calculated factor of safety curves show similar nonlinear trends for the different centrifuge models. Similar patterns for the factors of safety versus *g*-level curves were also obtained for the centrifuge models in the D- and S-series. The predicted *g*-level at failure for each model was determined as the *g*-level that yields a factor of safety of unity.

Fig. 13 shows a comparison between the *g*-levels at failure obtained experimentally for each centrifuge test and the values predicted using limit equilibrium analysis. The results show very good agreement between measured and predicted *g*-levels at failure, with all the points falling essentially on the 45° line. Based on the very good comparison between analytical and experimental results, it may be inferred that the limit equilibrium method is capable of accurately predicting the failure of the reinforced slopes. This good match also provides confidence in the selection of parameters (e.g., use of peak soil shear strength) and in the modeling assumptions (e.g., use of a uniform distribution of reinforcement forces with depth) made in the limit equilibrium analyses. Equally good comparisons between predicted and measured results were obtained for centrifuge slope models built using different reinforcement spacings, different soil densities, and model geotextiles with different ultimate tensile strengths.

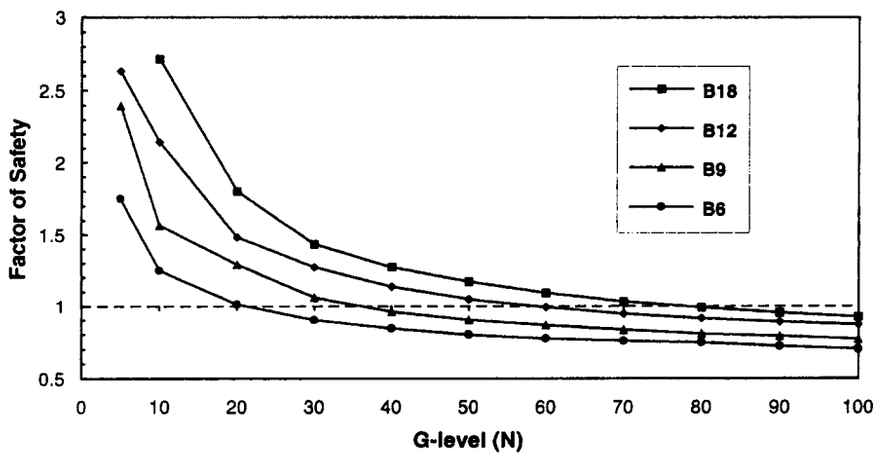

FIG. 12. Calculated Factors of Safety with Increasing *g*-Level for Models in B-Series

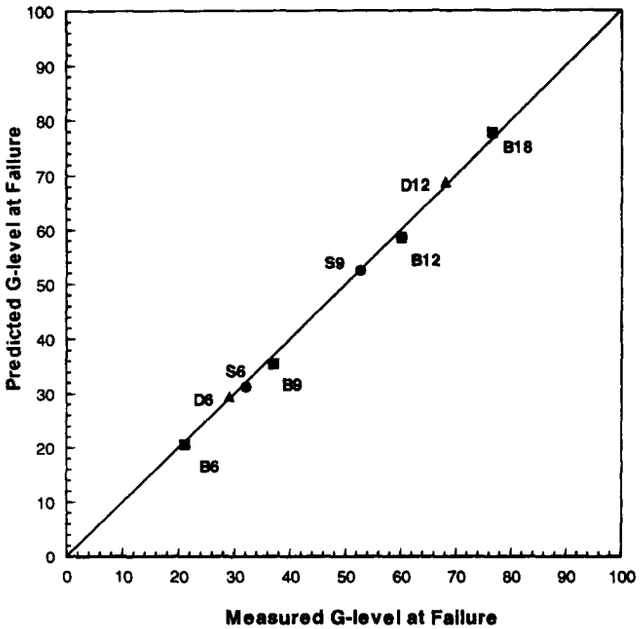

FIG. 13. Predicted and Measured *g*-Levels Causing Failure for All Centrifuge Models

Experimental and Predicted Location of Failure Surfaces

Correct identification of the location of the potential failure surfaces is relevant for the design of reinforced soil structures as it influences the required length of the reinforcements. The anchorage length required to provide enough pullout resistance is estimated as the reinforcement length beyond the potential failure surface. Although conventional design assumes that the location of the potential failure surface can be defined from limit equilibrium analysis, experimental evidence to substantiate this design procedure is, at best, limited.

Fig. 11(b) presents a comparison between the experimental and predicted locations of the failure surface for model B18. Similar comparisons were made for the rest of the models from the B-series, as well as for the models from the D- and S-series. Fig. 14 shows these comparisons for models D12 and S9. The figures show the location of the failure surfaces obtained experimentally from the tears on the geotextiles retrieved after testing and from the images recorded through the Plexiglas side wall during testing. Overall, there is an excellent agreement between the critical circles predicted by the limit equilibrium analyses and the two different experimental sources of information.

Evaluation of the failure surfaces obtained experimentally for the different models indicated that all centrifuge models failed along approximately the same failure surface (Zornberg et al. 1998). This observation is also true for the analytical results obtained from limit equilibrium analyses. Fig. 15 shows the location of the critical circles obtained from the analyses of the models in this study, performed using the experimental *g*-levels that brought each model to failure. In conclusion, the experimentally obtained failure surfaces matched the locations predicted by limit equilibrium for all centrifuge slope models. Equally good comparisons were obtained for centrifuge slope models built using different reinforcement spacings, different soil densities, and model geotextiles with different tensile strengths.

Evaluation of In-Soil Geotextile Tensile Strength

Centrifuge tests on reinforced slope models can be considered special tests for evaluating the in-soil mechanical properties of geosynthetics. This is because the conditions imposed on the geotextile reinforcements duplicate the operational conditions of prototype structures. A parametric evaluation was performed in which the factors of safety for all the centrifuge models were calculated using increasing values of geotextile tensile strength. The analyses were performed using the *g*-level at failure N_f obtained experimentally for each centrifuge test. Consequently, the estimated in-soil geotextile tensile strength for each model is the value that yields a factor of safety of one.

Fig. 16 shows the calculated factors of safety with increasing reinforcement tensile strength. The results obtained for all centrifuge models built using the same type of geotextile essentially collapse onto a single curve. As a unique in-soil geotextile tensile strength can be obtained from the different centrifuge models for each geotextile type, confidence can be placed in the in-soil geotextile tensile strength values adopted in the analyses. It is worth noting that the Factor of Safety versus tensile strength curve is very sensitive to the *g*-level at which the analysis is performed. This can be observed in Fig. 8 for analyses performed at different *g*-levels for the same model (model B18). The results shown in Fig. 16 also indicate no evidence of change of the in-soil geotextile tensile strength

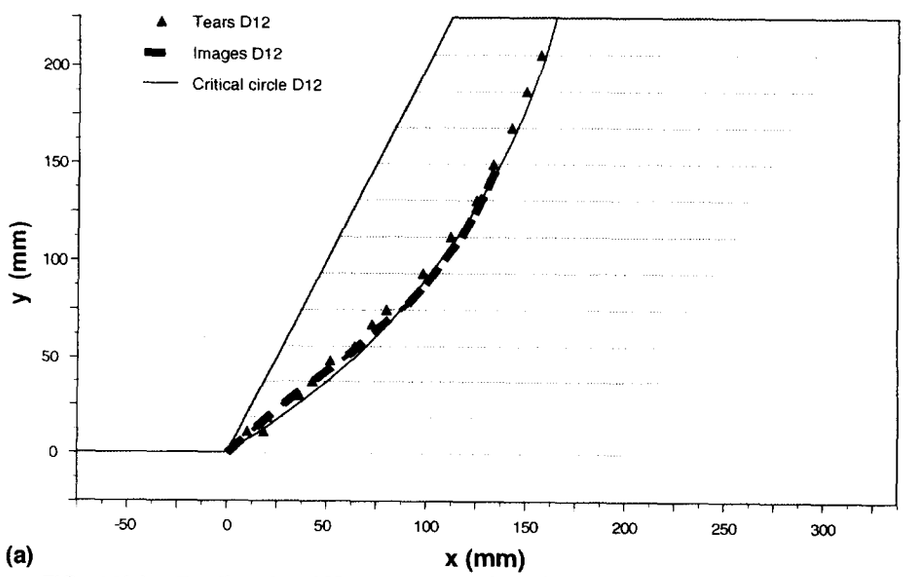

FIG. 14(a). Predicted and Measured Location of Failure Surface for Model D12

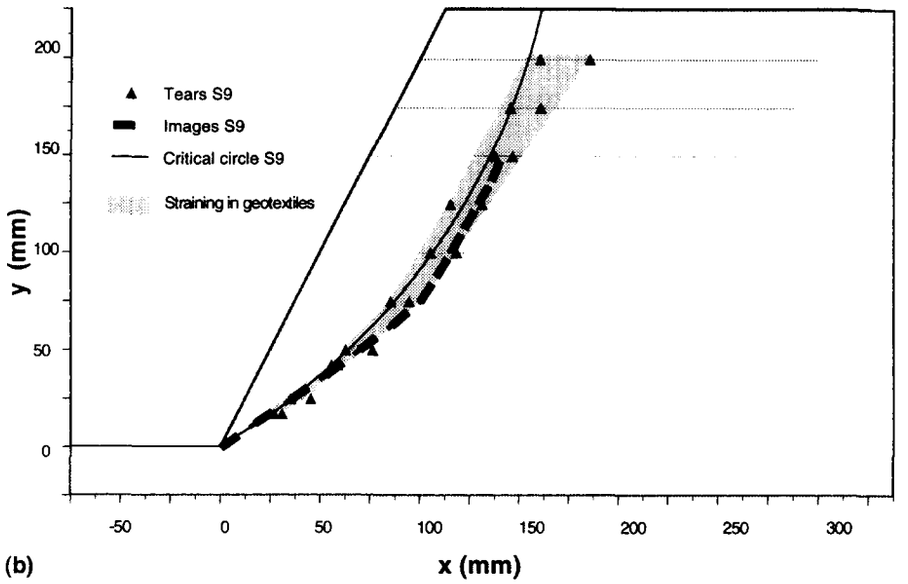

FIG. 14(b). Predicted and Measured Location of Failure Surface for Model S9

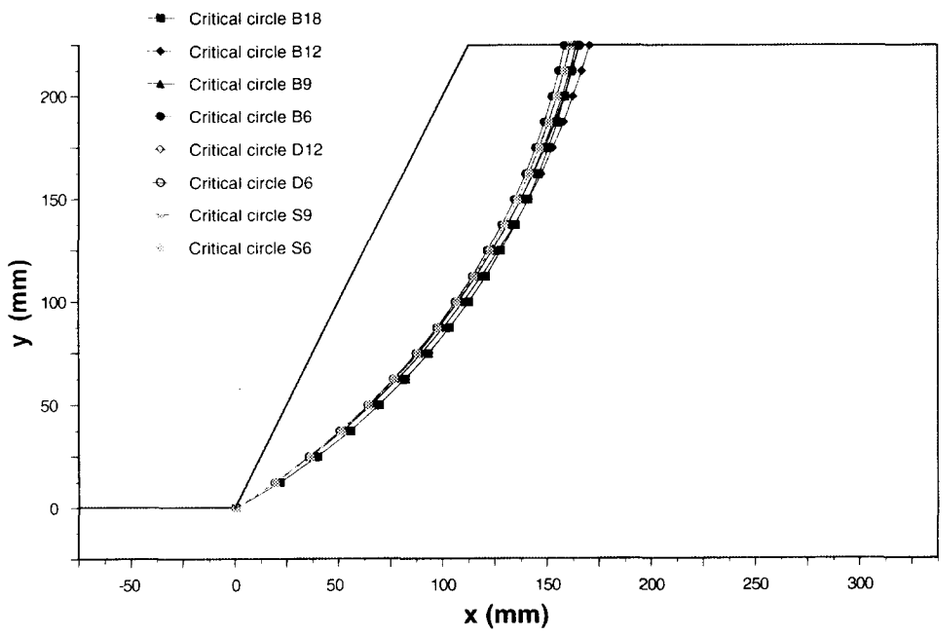

FIG. 15. Critical Circles Predicted by Limit Equilibrium for All Centrifuge Models

for models failing at significantly different accelerations. This suggests that the strength improvement of the geotextiles embedded in soil is not sensitive to the confining pressures, at least for the range of pressures for the models in this study. This evidence is consistent with the observation that improvement of mechanical properties of geotextiles embedded in soil is induced by the restraint of lateral deformations and not be the increase in confining pressures.

NORMALIZATION OF TEST RESULTS

Although design of geosynthetic reinforced slopes is commonly based on limit equilibrium methods, working stress design methods have been developed particularly for the analysis of reinforced soil vertical walls. Working stress design methods rely upon assumptions regarding the state of stress within the soil. Specifically, the horizontal soil stress distribution along the potential failure surface is defined based on the knowledge of an earth pressure coefficient, K. Tension in the reinforcements is then conventionally estimated from local equilibrium between horizontal soil stresses and reinforcement forces. The value of the coefficient K has been determined semiempirically and, for the case of vertical walls with extensible reinforcements and horizontal backfill, it has been assumed to be the active earth coefficient K_a that depends only on the soil friction angle ϕ.

In the case of geosynthetic reinforced soil slopes, equilibrium should also be satisfied between reinforcement forces and horizontal soil stresses along the potential failure surface. It can then be postulated that the horizontal soil stresses along the potential failure surface can be characterized by a global earth pressure coefficient K. Such a coefficient K would not depend only on the soil friction angle ϕ, but also on the slope inclination β. The following global equilibrium equation should then apply at the moment of failure:

$$\mathrm{RTS}_{ult}(\phi, \beta) = \frac{1}{2} K(\phi, \beta)\gamma H^2 \tag{4}$$

where RTS_{ult} (ϕ, β) = Reinforcement Tension Summation at

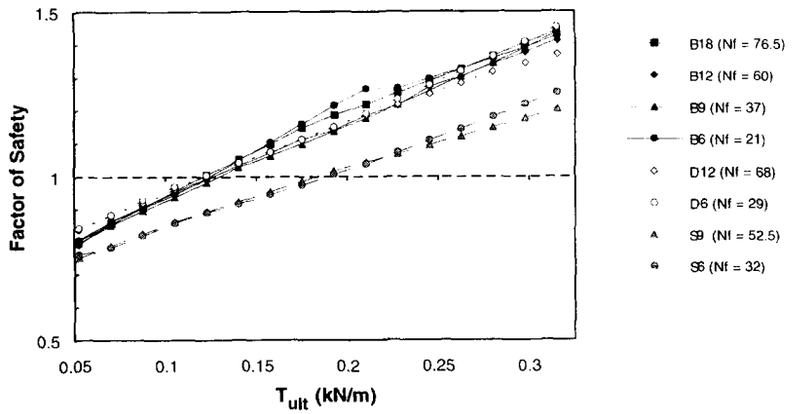

FIG. 16. Effect of Geotextile Tensile Strength on Calculated Factor of Safety for All Centrifuge Models

the moment of failure; γ = soil unit weight; and H = slope height. The earth pressure coefficient $K(\phi, \beta)$ can then be interpreted from (4) as a Normalized Reinforcement Tension Summation:

$$K(\phi, \beta) = \text{RTS}_{ult}(\phi, \beta)\left(\frac{2}{\gamma H^2}\right) \tag{5}$$

The use of the coefficient 1/2 in (4) is consistent with the traditional assumption of a triangular distribution of horizontal stresses along the potential failure surface. However, independent of the assumed distribution of horizontal stresses with depth, (4) states more generically that the Reinforcement Tension Summation is proportional to the soil unit weight γ and to the square of the slope height H.

Assuming that all reinforcements achieve the ultimate load T_{ult} simultaneously, as inferred from the centrifuge experimental results, the Normalized Reinforcement Tension Summation $K(\phi, \beta)$ can be estimated as

$$K(\phi, \beta) = n\, T_{ult}\left(\frac{2}{\gamma H^2}\right) \tag{6}$$

where n = number of reinforcements. Dimensionless coefficients similar to $K(\phi, \beta)$ have been previously used in order to develop design charts for geosynthetic reinforced soil slopes (Schmertmann et al. 1987; Leshchinsky and Boedeker 1989; Jewell 1991). The validity of the proposed normalization of the summation of reinforcement forces can be investigated from the centrifuge results of this study. For a reinforced slope model that failed at an acceleration equal to N_f times the acceleration of gravity, the coefficient $K(\phi, \beta)$ can be estimated considering the increase in unit weight:

$$K(\phi, \beta) = n\, T_{ult} \cdot \left(\frac{2}{\gamma H^2}\right) \cdot \frac{1}{N_f} \tag{7}$$

In addition to the number of primary reinforcement layers, the value of n used in (7) includes the number of overlaps that were intersected by the failure surface in the centrifuge slope models. All centrifuge slope models were built with the same slope inclination β. Consequently, if the suggested normalization holds true, a single coefficient $K(\phi, \beta)$ should be obtained for all models built with the same backfill. That is, a single coefficient should be obtained for all models built with Monterey No. 30 sand placed at the same relative density.

Fig. 17 shows the centrifuge results in terms of $(nT_{ult})(2/\gamma H^2)$ versus the g-level at failure N_f. The results in the figure clearly show that a linear relationship can be established for all models built using the same sand relative density. As inferred from (7), the slope of the fitted line corresponds to the Normalized RTS coefficient $K(\phi, \beta)$. The results obtained using the centrifuge models from the B- and S-series, built

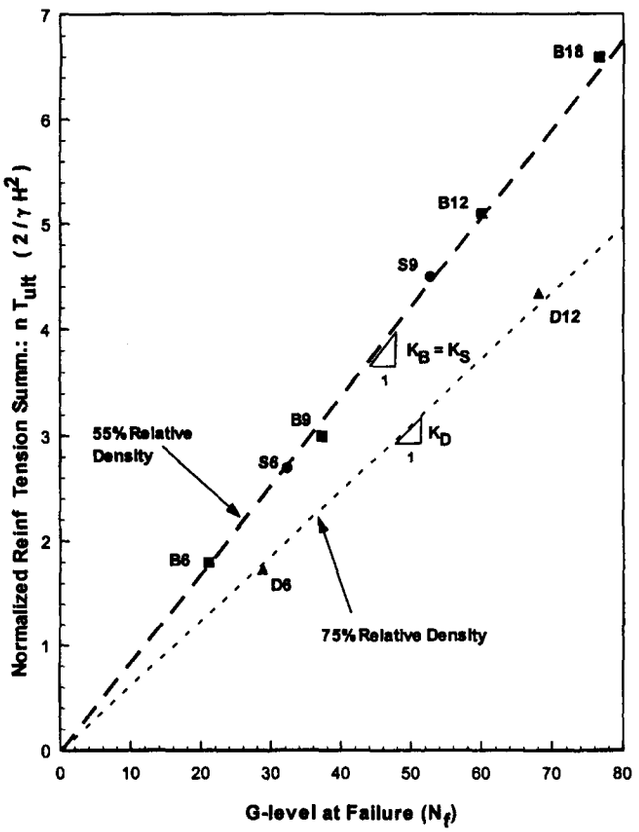

FIG. 17. Normalized Reinforcement Tension Summation (RTS) Values from Centrifuge Test Results

using Monterey sand placed at 55% relative density, define a normalized coefficient $K(\phi, \beta) = K_B = K_S = 0.084$. Similarly, centrifuge results from the D-series models, built using Monterey sand at 75% relative density, define a normalized coefficient $K(\phi, \beta) = K_D = 0.062$. Consequently, the centrifuge test results show that the Reinforcement Tension Summation can be normalized and that the normalized coefficient depends on the soil friction angle and on the slope inclination. These results provide sound experimental evidence supporting the use of charts based on normalized coefficients for preliminary design of geosynthetic reinforced slopes.

ADDITIONAL REMARKS AND COMPARISONS

To further evaluate the predictive capabilities of limit equilibrium methods, the centrifuge experimental results were compared to predictions based on methods proposed by Leshchinsky and Boedeker (1989) and Jewell (1991). These meth-

ods have been presented in design charts for a range of structure geometries and soil parameters suitable for the analysis of the centrifuge slope models.

The design charts have similar characteristics: the overall factor of safety is accounted for by using a factored soil friction angle which, together with the slope inclination, yields the required summation of reinforcement forces. Validation of the centrifuge model results can be done using the design charts in the reverse order, i.e., for a given summation of reinforcement forces the mobilized friction angle can be estimated. As the analysis is performed for centrifuge models at failure (FS = 1), the mobilized friction angle obtained from the design charts should equal the peak soil friction angle. Leshchinsky and Boedeker (1989) and Jewell (1991) consider a triangular distribution of the reinforcement forces, with maximum tension at the base of the slope. This distribution is not in agreement with the experimental centrifuge results and has not been adopted in the limit equilibrium analyses performed herein. Nevertheless, the design charts can also be used for the case of uniform distribution of reinforcement forces with depth.

Leshchinsky and Boedeker (1989) use a logarithmic spiral failure mechanism to obtain the minimum factor of safety for reinforced slopes, while satisfying all three global equilibrium equations. Fig. 18(a) shows the design chart for the required tensile force in the reinforcements. The coefficient m in the chart defines the slope inclination (m = 2 for a 1H:2V slope). For the case of uniform distribution of reinforcement forces with depth, the dimensionless mobilized equivalent tensile resistance T_m in the chart equals the Normalized RTS coefficient $K(\phi, \beta)$. The Normalized RTS coefficients (K_D and $K_B = K_S$) have been obtained from Fig. 17 for each series. The mobilized friction angles ϕ_m obtained using these normalized coefficients are $\phi_m \approx 39°$ and $\phi_m \approx 42°$ for centrifuge models built with sand at 55 and 75% relative densities, respectively. These predicted mobilized friction angles are in good agreement with the peak plane strain friction angles obtained for Monterey sand at the relative densities used in the centrifuge

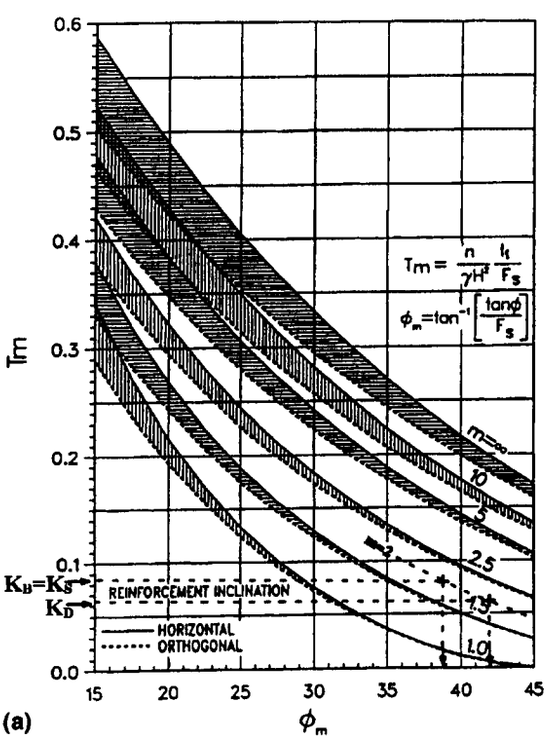

FIG. 18(a). Design Chart for Reinforced Soil Slopes (Leshchinsky and Boedeker 1989)

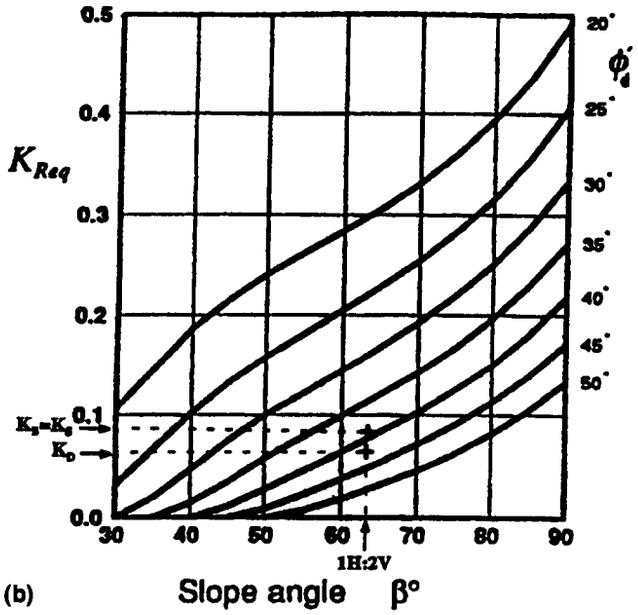

FIG. 18(b). Design Chart for Reinforced Soil Slopes (Jewell 1991)

models (ϕ_{ps} = 39.5° and ϕ_{ps} = 42.5°). Consequently, the predicted factors of safety are approximately 1.00, which indicates good agreement with the experimental results.

Jewell (1991) presented an approach for the design of geosynthetic reinforced slopes using a two-part wedge analysis. The total required reinforcement tensile forces can be estimated using the design chart presented in Fig. 18(b). The coefficient K_{req} in the design chart is equivalent to the Normalized RTS coefficient $K(\phi, \beta)$, ϕ_d is the design friction angle of the backfill soil, and β is the slope inclination. Using the normalized coefficients obtained from the centrifuge tests (K_D and $K_B = K_s$), the design friction angles ϕ_d obtained for a slope angle β = 63.4° (1H:2V) are $\phi_d \approx 39°$ and $\phi_d \approx 42.5°$ for centrifuge models built with sand at 55 and 75% relative densities, respectively. The predicted design fricton angles are in very good agreement with the peak plane strain friction angles obtained for Monterey sand at the relative densities used in the models. Consequently, Jewell's limit equilibrium design methodology also shows good agreement with the experimental results.

The good comparisons between experimental centrifuge data and predictions using different limit equilibrium methodologies suggest that confidence can be placed on the ability of limit equilibrium methods to analyze the stability of geosynthetic reinforced slopes. It should be noted, though, that this study focused only on one of the failure modes contemplated in the design of geosynthetic reinforced slopes (internal failure due to the breakage of the reinforcements). Moreover, this study concentrated specifically on the performance of slopes reinforced using geotextile reinforcements. Although it seems reasonable to extend the validity of the conclusions to slopes reinforced with other extensible reinforcements, these conclusions should not be extrapolated to slopes reinforced with inextensible inclusions without careful evaluation.

CONCLUSIONS

Using the centrifuge modeling technique, a series of geotextile reinforced soil slope models was tested to failure in order to identify the possible failure mechanisms and to verify the ability of limit equilibrium methods to predict the experimental results. The variables considered in the centrifuge study were the reinforcement spacing, the reinforcement tensile

strength, and the soil shear strength, which can all be taken into account using limit equilibrium analyses. A testing program was initially undertaken to evaluate the strength properties under operational conditions of the sand used as backfill material, the geotextile reinforcements, and the several interfaces in the slope models. The tensile strength of the model geotextiles was found to depend on the testing boundary conditions.

The effect of different modeling assumptions on the calculated factors of safety was investigated by performing parametric limit equilibrium studies. Based on the interpretation of the experimental results on the performance of the reinforced slope models at failure [see Zornberg et al. (1998)], the peak soil shear strength (instead of the critical state shear length) and a uniform distribution of maximum reinforcement forces with depth (instead of a conventional triangular distribution) were adopted in these analyses. The suitability of limit equilibrium methods for the analysis of geosynthetic reinforced slopes was then evaluated by comparing experimental results and analytical predictions. The following conclusions can be drawn from this evaluation:

- Very good agreement was obtained between the experimental g-levels at failure obtained for the centrifuge models and the results predicted by limit equilibrium.
- Equally good agreement was obtained between the locations of the failure surface obtained experimentally and the locations of the critical circular failure surface predicted by limit equilibrium.
- Experimental observations and the good agreement between experimental and predicted results indicate that the orientation of the reinforcement forces should be considered horizontal in the analysis of reinforced soil slopes.
- Important contribution to the stability of the reinforced slope models was provided by the overlapping reinforcement layers.
- Different rigorous limit equilibrium methodologies evaluated in this paper were found to provide equally good results.
- The centrifuge test results provided insight into the evaluation of in-soil tensile strength of geotextiles and suggest that in-soil improvement of geotextile mechanical properties is induced mainly by the restriction of lateral deformations.
- Consistency of the centrifuge results was observed by the fact that all centrifuge slope models built using the same backfill soil yielded a single Normalized Reinforcement Tension Summation coefficient. The normalization of the experimental results into dimensionless coefficients supports the use of charts for preliminary design of geosynthetic reinforced slopes.

Overall, centrifuge testing provided much needed evidence that limit equilibrium methodologies adequately predict the performance of geosynthetic reinforced soil structures at failure.

ACKNOWLEDGMENTS

Funding for this study has been provided by the California State Department of Transportation under project number RTA65T128. Lili Nova-Roessig performed the laboratory tests on Monterey Sand. This assistance is gratefully acknowledged. Support received by the first writer from CNPq (National Council for Development and Research, Brazil) is also greatly appreciated.

APPENDIX I. REFERENCES

Bishop, A. W. (1955). "The use of the slip circle in stability analysis of slopes." *Géotechnique*, London, U.K., 5(1), 7–17.

Bolton, M. (1986). "The strength and dilatancy of sands." *Géotechnique*, London, U.K., 36(1), 65–78.

Correia, R. M. (1988). "A limit equilibrium method for slope stability analysis." *Proc., 5th Int. Symp. Landslides*, A. A. Balkema, Rotterdam, The Netherlands, 595–598.

Duncan, J. M. (1996). "State-of-the-art: Limit equilibrium and finite element analysis of slope." *J. Geotech. Engrg.*, ASCE, 122(7), 577–596.

Espinoza, R., Repetto, P., and Muhunthan, B. (1992). "General framework for stability analysis of slopes." *Géotechnique*, London, U.K., 42(4), 603–615.

Fellenius, W. (1936). "Calculation of the stability of earth dams." *Proc., 2nd Congr. Large Dams*, Vol. 4, Washington, D.C., 445–462.

Jaber, M. B. (1989). "Behavior of reinforced soil walls in centrifuge model tests," PhD dissertation, Dept. of Civ. Engrg., University of California, Berkeley, Calif.

Janbu, N. (1954). "Applications of composite slip surface for stability analysis." *Proc., Eur. Conf. on Stability of Earth Slopes*, Vol. 3, Stockholm, Sweden, 43–49.

Jewell, R. A. (1990). "Strength and deformation in reinforced soil design." *Proc., 4th Int. Conf. on Geotextiles, Geomembranes and Related Products*, International Geotextile Society, The Hague, The Netherlands, 913–946.

Jewell, R. A. (1991). "Application of revised design charts for steep reinforced slopes." *Geotextiles and Geomembranes*, 10, 203–233.

Kulhawy, F. H., and Mayne, P. W. (1990). "Manual on estimating soil properties for foundation engineering." *Rep. EL-6800*, Electric Power Research Institute, Palo Alto, Calif.

Ladd, C., Foott, R., Ishihara, K., Schlosser, F., and Poulos, H. (1977). "Stress-deformation and strength characteristics." *Proc., 9th Int. Conf. on Soil Mech. and Found. Engrg.*, A. A. Balkema, Rotterdam, The Netherlands, 421–494.

Lade, P., and Duncan, J. M. (1973). "Cubical triaxial tests on cohesionless soil." *J. Soil Mech. and Found. Div.*, ASCE, 99(10), 793–812.

Leflaive, E., Paute, J., and Segouin, M. (1982). "Strength properties measurement for practical applications." *Proc., 2nd Int. Conf. on Geotextiles*, International Geotextile Society, Las Vegas, Nev., 733–738.

Leshchinsky, D., and Boedeker, R. H. (1989). "Geosynthetic reinforced soil structures." *J. Geotech. Engrg.*, ASCE, 115(10), 1459–1478.

Li, X. S., Chan, C. K., and Shen, C. K. (1988). "An automated triaxial testing system." *Advanced triaxial testing of soil and rock, ASTM STP 977*, ASTM, Philadelphia, Pa., 95–106.

Ling, H. I., Wu, J. T. H., and Tatsuoka, F. (1992). "Short-term strength and deformation characteristics of geotextiles under typical operational conditions." *Geotextiles and Geomembranes*, 11(2), 185–219.

Lowe, J., and Karafiath, L. (1960). "Stability of earth dams upon drawdown." *Proc., 1st Panamerican Conf. of Soil Mech.*, Vol. 2, Mexico City, Mexico, 537–552.

Marachi, N., Duncan, J. M., Chan, C., and Seed, H. B. (1981). "Plane-strain testing of sand." *Laboratory shear strength of soil, ASTM STP 740*, ASTM, Philadelphia, Pa., 294–302.

McGown, A., Andrawes, K. Z., and Kabir, M. H. (1982). "Load-extension testing of geotextiles confined in soil." *Proc., 2nd Int. Conf. on Geotextiles*, International Geotextile Society, Las Vegas, Nev., 793–798.

Mitchell, J. K., Seed, R. B., and Seed, H. B. (1990). "The Kettleman Hills waste landfill slope failure—I: Liner interface properties." *J. Geotech. Engrg.*, ASCE, 116(4), 647–668.

Morgenstern, N. R., and Price, V. E. (1965). "The analysis of the stability of general slip surfaces." *Géotechnique*, London, U.K., 15, 70–93.

Resl, S. (1990). "Soil-reinforcing mechanisms of non woven geotextiles." *Proc., 4th Int. Conf. on Geotextiles, Geomembranes and Related Products*, The Hague, The Netherlands, 93–96.

Riemer, M. F. (1992). "The effects of testing conditions on the constitutive behavior of loose, saturated sand under monotonic loading," PhD dissertation, Dept. of Civ. Engrg., University of California, Berkeley, Calif.

Sarma, S. K. (1973). "Stability analysis of embankments and slopes." *Géotechnique*, London, U.K., 23(3), 423–433.

Sarma, S. K. (1979). "Stability analysis of embankments and slopes." *J. Geotech. Engrg., Div.*, ASCE, 105(2), 1511–1524.

Schlosser, F., and Vidal, H. (1969). "La terre armee." *Bull. Liaison du Laboratorie Central des Ponts et Chaussees*, Paris, France, 41, 101–144.

Schmertmann, G. R., Chouery-Curtis, V. E., Johnson, R. D., and Bonaparte, R. (1987). "Design charts for geogrid-reinforced soil slopes." *Proc., Geosynthetics '87 Conf.*, New Orleans, La., 108–120.

Shewbridge, S., and Sitar, N. (1989). "Deformation characteristics of reinforced sand in direct shear." *J. Geotech. Engrg.*, ASCE, 115(8), 1134–1147.

Shrestha, S., and Bell, J. (1982). "A wide strip tensile test of geotextiles."

Proc., 2nd Int. Conf. on Geotextiles, International Geotextile Society, Las Vegas, Nev., 739–744.
Spencer, E. (1967). "A method of analysis of the stability of embankments assuming parallel inter-slice forces." *Géotechnique*, London, U.K., 24(4), 661–665.
Terzaghi, K. (1956). *Theoretical soil mechanics*. John Wiley & Sons, Inc., New York, N.Y.
Wright, S. G. (1990). *UTEXAS3 A computer program for slope stability calculations*. Shinoak Software, Austin, Tex.
Wright, S. G., and Duncan, J. M. (1991). "Limit equilibrium stability analyses for reinforced slopes." *Transp. Res. Record 1330*, Transportation Research Board, Washington, D.C., 40–46.
Zornberg, J. G., and Mitchell, J. K. (1994). "Finite element prediction of the performance of an instrumented geotextile-reinforced wall." *Proc., 8th Int. Conf. of the Int. Assn. for Comp. Methods and Adv. in Geomechanics (IACMAG '94)*, Vol. 2, A. A. Balkema, Rotterdam, The Netherlands, 1433–1438.
Zornberg, J. G., Sitar, N., and Mitchell, J. K. (1995). "Performance of geotextile-reinforced soil slopes at failure: A centrifuge study." *Geotech. Res. Rep. No. UCB/GT/95-01*, Dept. of Civ. Engrg., University of California, Berkeley, Calif.
Zornberg, J. G., Sitar, N., and Mitchell, J. K. (1998). "Performance of geosynthetic reinforced slopes at failure." *J. Geotech. and Geoenvironmental Engrg.*, ASCE, 124(8), 670–683.

APPENDIX II. NOTATION

The following symbols are used in this paper:

FS = factor of safety (dimensionless);
f = interface friction factor (dimensionless);
g = acceleration of gravity (m^2/s);
H = slope height (m);
K = earth pressure coefficient, normalized RTS coefficient (dimensionless);
K_a = active earth pressure coefficient (dimensionless);
K_B = normalized RTS for models in B-series (dimensionless);
K_D = normalized RTS for models in D-series (dimensionless);
K_{req} = required reinforcement tensile forces coefficient (Jewell 1991) (dimensionless);
K_S = normalized RTS for models in S-series (dimensionless);
N = g-level imparted to a centrifuge model (dimensionless);
N_f = g-level at failure (dimensionless);
n = number of reinforcement layers (dimensionless);
RTS = Reinforcement Tension Summation (kN/m);
RTS_{ult} = Reinforcement Tension Summation at moment of failure (kN/m);
T_m = mobilized equivalent tensile resistance (Leshchinsky and Boedeker 1989) (dimensionless);
T_{ult} = reinforcement tensile strength (kN/m);
β = slope inclination (degrees);
γ = soil unit weight (kN/m^3);
δ = interface friction angle (degrees);
ϕ = soil friction angle (degrees);
ϕ_{cs} = critical state friction angle (degrees);
ϕ_d = design friction angle (Jewell 1991) (degrees);
ϕ_m = mobilized friction angle (Leshchinsky and Boedeker 1989) (degrees);
ϕ_{ps} = plane strain friction angle (degrees); and
ϕ_{tc} = triaxial compression friction angle (degrees).